

Low-Energy Electron-Induced Chemistry of CF₂Cl₂: Implications for the Ozone Hole?

Nozomi Nakayama, Stephen C. Wilson, Laura E. Stadelmann, Hsiao-Lu D. Lee, Casey A. Cable, and Christopher R. Arumainayagam*

Department of Chemistry, Wellesley College, Wellesley, Massachusetts 02481

Received: December 15, 2003

We report on the first direct investigation of the low-energy electron-induced production of neutral species from the chlorofluorocarbon CF₂Cl₂, commonly known as Freon-12 or CFC-12. Our experiments were motivated by a newly proposed hypothesis, which suggests that low-energy electrons produced by cosmic rays, in addition to UV-vis photons from the sun, interact with chlorofluorocarbons to produce chlorine atoms that subsequently destroy ozone in the Antarctic. Our experimental procedure involves low-energy (5–100 eV) electron irradiation of nanoscale thin films (~10 Å thickness) of CF₂Cl₂ grown at 100 K on a molybdenum single crystal in an ultrahigh vacuum chamber ($p \sim 1 \times 10^{-10}$ Torr). Post-irradiation temperature-programmed desorption experiments were used to identify C₂F₄Cl₂, C₂F₃Cl₃, C₂F₂Cl₄, C₂F₃Cl, C₂F₂Cl₂, and C₂F₄ as electron-induced radiolysis products of CF₂Cl₂. In contrast to previous studies of *photon*-induced dissociation, our studies of *electron*-induced dissociation demonstrate facile C–F bond cleavage in CF₂Cl₂. This finding may have implications for understanding the partitioning of Cl and F among source, sink, and reservoir gases in the stratosphere.

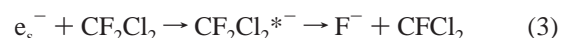
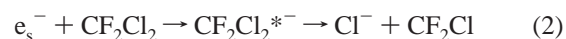
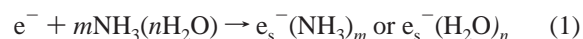
1. Introduction

Photon-induced dissociation of chlorofluorocarbons (CFCs) has been widely accepted as the mechanism for the formation of Cl atoms which are known to deplete stratospheric ozone.¹ Even though the cross-sections for electron-induced dissociation of chlorofluorocarbons are known to be several orders of magnitude higher than those of photon-induced dissociation,² electron-induced dissociation processes of chlorofluorocarbons have been considered to be insignificant in the stratosphere because the *free* electron density in the stratosphere is very low.³ However, recent studies have shown that electron-induced dissociation processes of chlorofluorocarbons may be important in the production of Cl atoms in polar stratospheric clouds (PSCs) containing water ices in which low-energy *solvated* electrons are known to be found.^{4–6} According to this hypothesis, Cl[–] ions resulting from the electron-induced dissociation of chlorofluorocarbons interact with sunlight yielding Cl atoms which then react with the ozone producing O₂ and O.

The study of dichlorodifluoromethane (CF₂Cl₂), commonly known as CFC-12 or Freon-12, is of interest because it is the most important chlorofluorocarbon responsible for stratospheric ozone depletion in the Antarctic region. To investigate the role of electrons in producing chlorine atoms in the polar stratospheric clouds, Lu and Madey conducted experiments with CF₂Cl₂ coadsorbed with water and ammonia. They demonstrated a very large enhancement (up to a factor of 10⁴) in the electron-stimulated desorption of Cl[–] from CF₂Cl₂ when submonolayer coverages of CF₂Cl₂ were coadsorbed with polar water or ammonia.^{4,5} In contrast, when CF₂Cl₂ was coadsorbed with nonpolar molecules such as CH₄, only small enhancements were observed.^{6,7}

According to the original proposal of Lu and Madey, the low-energy secondary electrons can be efficiently solvated in clusters of molecules with permanent dipole moments such as water.

These solvated electrons can then tunnel from the water clusters to the CF₂Cl₂ present on ice surfaces causing vibrational excitation followed by dissociation of CF₂Cl₂.⁵ Lu and Madey described the process as follows:



where e_s^- represents a solvated electron and CF₂Cl₂[–] represents the vibrationally excited intermediate.

On the basis of measuring electron trapping coefficients using the low-energy electron transmission (LEET) method, Lu and Sanche subsequently demonstrated that it is presolvated electrons rather than solvated electrons in H₂O or NH₃ that are responsible for the enhancement in the electron-induced dissociation of CF₂Cl₂.⁸ According to Lu and Sanche, electrons in the precursor state of the solvated state are transferred to CF₂Cl₂ causing dissociation via dissociative electron attachment (DEA).

On the basis of these findings, a new path for ozone depletion has been proposed: (1) cosmic rays produce an abundance (~4 × 10⁴ electrons per MeV of energy deposited)⁹ of low-energy electrons that may become trapped in precursor states in the water ices present in polar stratosphere clouds; (2) these near-zero energy electrons transfer rapidly to chlorofluorocarbons causing dissociation to produce chloride ions; and (3) photo-detachment of these chloride ions yields chlorine atoms that destroy ozone in the Antarctic region.⁹

Several pieces of evidence were advanced to support the claim that it is the low-energy electrons produced by cosmic radiation that are responsible for ozone depletion: (1) cosmic radiation is strongest at altitudes of 15–18 km in the stratospheric atmosphere and at the poles of the Earth, both regions where ozone depletion is most pronounced, and (2) during the 11-

* Address correspondence to this author. Phone: 781-283-3326. Fax: 781-283-3642. E-mail: carumain@wellesley.edu.

year cosmic ray cycle, which is in inverse phase to the solar activity cycle, the lowest concentration of ozone is observed when the cosmic ray flux is the highest.⁹ However, the role of cosmic radiation in the production of the ozone hole remains an unresolved issue.^{10–12}

We have used the results of postirradiation temperature-programmed desorption (TPD) experiments to (1) identify the radiolysis products of CF_2Cl_2 resulting from low-energy electron irradiation and (2) probe the dependence of radiolysis product yield on electron fluence and electron energy. The interactions of electrons with CF_2Cl_2 have been studied previously with other techniques.^{13–18} On the basis of the measurements of electron stimulated desorption yields and kinetic energy distributions for Cl^- anions from thin films of CF_2Cl_2 , the electron-induced synthesis of molecular Cl_2 was deduced.¹⁵ Our results demonstrate that (1) electron-induced reactions of condensed CF_2Cl_2 yield $\text{C}_2\text{F}_4\text{Cl}_2$, $\text{C}_2\text{F}_3\text{Cl}_3$, $\text{C}_2\text{F}_2\text{Cl}_4$, $\text{C}_2\text{F}_3\text{Cl}$, $\text{C}_2\text{F}_2\text{Cl}_2$, and C_2F_4 as radiolysis products, providing evidence for both C–Cl and C–F bond cleavage, and (2) $\text{C}_2\text{F}_4\text{Cl}_2$, $\text{C}_2\text{F}_3\text{Cl}_3$, and $\text{C}_2\text{F}_2\text{Cl}_4$ form as a result of two independent dissociation events.

2. Experimental Section

Postirradiation temperature-programmed desorption (TPD) experiments were conducted in a custom-designed stainless steel ultrahigh vacuum (UHV) chamber ($p \sim 1 \times 10^{-10}$ Torr) described in detail previously.¹⁹ The temperature of the crystal was measured with a W-5% Re vs W-26% Re thermocouple spot-welded to the crystal. Prior to every postirradiation temperature-programmed desorption experiment, the Mo(110) single crystal was cleaned by dosing oxygen at a surface temperature of ~ 1300 K and subsequently heating the crystal briefly to ~ 2200 K by electron bombardment. Removal of carbon contamination is accomplished by this procedure because the reaction of oxygen with carbon on the surface produces gaseous CO at 1300 K. The excess oxygen is removed by heating the crystal to 2200 K, above the desorption temperature of oxygen. Low-energy electron diffraction (LEED) was used to verify the long-range order of the Mo(110) surface.

Gaseous CF_2Cl_2 purchased from SynQuest Labs (lot assay of 99.8% purity) was dosed on the crystal at ~ 100 K, using a direct doser with a precision leak valve (Vacuum Generators MD7), to obtain a multilayer coverage of CF_2Cl_2 (~ 2 monolayers). To reduce the effect of surface charging, film thickness was minimized to decrease the distance to the conducting metal surface. The amount of CF_2Cl_2 dosed onto the crystal was quantified by the pressure drop in the gas-handling lines as measured by a capacitance manometer (MKS Baratron) capable of measuring pressure in Torr up to one part in 10 000. Temperature-programmed desorption experiments were used to estimate the coverage of CF_2Cl_2 . One monolayer (1 ML) is defined as the maximum exposure of CF_2Cl_2 that does not yield a multilayer peak.

The CF_2Cl_2 thin films were irradiated with electrons from the mass spectrometer filament (UTI Model 100C mass spectrometer). When an ionization energy of 70 eV was used during electron irradiation, an electron flux of $\sim 2 \times 10^{13} \text{ cm}^{-2} \text{ s}^{-1}$ (lower limit because scattered electrons are not counted) with an energy of 55 eV was obtained at the grounded crystal surface. Surface charging may result in an uncertainty of a few eV in our energy scale.

Following irradiation of the thin film, the crystal was heated radiatively at ~ 7 K/s to 700 K. As the crystal was heated, fragments of species desorbing from the surface as a function of temperature were detected with the UTI Model 100C mass

Post-Irradiation TPD of CF_2Cl_2

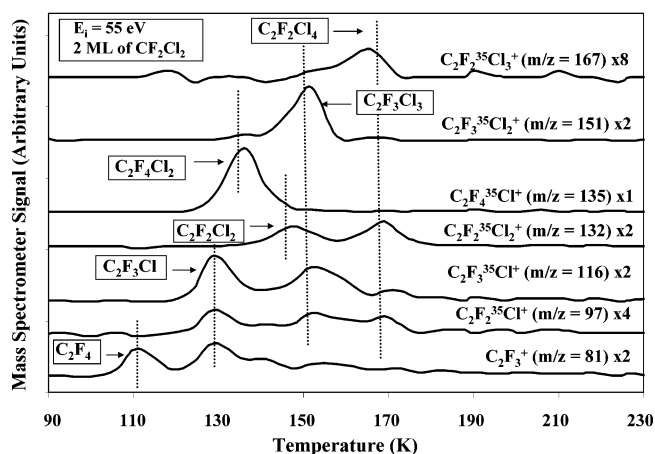


Figure 1. Postirradiation (55 eV electrons at a fluence of $1.5 \times 10^{15} \text{ cm}^{-2}$) temperature-programmed desorption data of CF_2Cl_2 multilayers (two layers) showing the desorption of C_2F_4 , $\text{C}_2\text{F}_3\text{Cl}$, $\text{C}_2\text{F}_2\text{Cl}_2$, $\text{C}_2\text{F}_4\text{Cl}_2$, $\text{C}_2\text{F}_3\text{Cl}_3$, and $\text{C}_2\text{F}_2\text{Cl}_4$.

spectrometer and thermocouple interfaced to a computer. The center of the crystal was aligned with the 1/8-in.-diameter aperture of the mass spectrometer shield to optimize the detection of the species desorbing from the center of the crystal. The ionization energy of the mass spectrometer was always set at 70 eV during thermal desorption experiments. A bias voltage of -100 V was applied to the crystal prior to turning on the mass spectrometer to prevent further electron irradiation. Typically 10 mass spectral fragments were monitored in a single experiment, and fragments up to m/z 300 were monitored to identify the radiolysis products of CF_2Cl_2 .

3. Results and Discussion

3.1. Identification of Radiolysis Products. Results of postirradiation temperature-programmed desorption (TPD) experiments were used to identify C_2F_4 , $\text{C}_2\text{F}_3\text{Cl}$, $\text{C}_2\text{F}_4\text{Cl}_2$, $\text{C}_2\text{F}_2\text{Cl}_2$, $\text{C}_2\text{F}_3\text{Cl}_3$, and $\text{C}_2\text{F}_2\text{Cl}_4$ as low-energy electron-induced radiolysis products of CF_2Cl_2 . These results demonstrate that low-energy electron-induced radiolysis of CF_2Cl_2 results in C–F bond cleavage, in addition to C–Cl bond cleavage. Interestingly, it has been demonstrated that C–F bond cleavage does not occur during UV–vis photolysis of CF_2Cl_2 .^{20,21}

We have previously demonstrated that temperature-programmed desorption experiments conducted following low-energy electron irradiation of multilayer thin films provide an effective method to investigate the effects of high-energy radiation, including radical–radical reactions.¹⁹ Electron-induced reaction products of CF_2Cl_2 were identified by using a combination of three methods: (1) comparing fragments found at a given temperature in the thermal desorption data to known mass spectra,²² (2) invoking trends in multilayer desorption temperatures and boiling points, and (3) comparing the results of postirradiation temperature-programmed desorption experiments to results of γ -radiolysis studies.

The results of postirradiation thermal desorption data are shown in Figure 1. For the sake of clarity, only a few mass spectral fragments that evinced a desorption peak are shown in this figure. The identification of the low-energy electron-induced radiolysis products based on postirradiation thermal desorption experiments is discussed in detail below.

A. Identification of C_2F_4 . Desorption peaks for m/z 81 (C_2F_3^+) (Figure 1) and 100 (C_2F_4^+) were observed at ~ 111 K in postirradiation temperature-programmed desorption experiments

and were assigned to the radiolysis product C_2F_4 , a species not identified in γ -radiolysis studies.^{23,24} The mass spectral fragment m/z 135 ($C_2F_4Cl^+$) does not have a peak at ~ 111 K, eliminating $C_2F_4Cl_2$ as a candidate. The absence of a peak for m/z 119 ($C_2F_5^+$) at ~ 111 K eliminates C_2F_6 as a possibility. Pentafluorochloroethane (C_2F_5Cl) was ruled out because m/z 135 ($C_2F_4Cl^+$) and 119 ($C_2F_5^+$) are both absent at ~ 111 K in the thermal desorption data. Moreover, the observed desorption temperature of C_2F_4 (~ 111 K) is below that of CF_2Cl_2 (~ 129 K), consistent with the boiling point trend: C_2F_4 (198 K) < CF_2Cl_2 (243 K).²²

B. Identification of C_2F_3Cl . Desorption peaks for m/z 118 ($C_2F_3^{37}Cl^+$), 116 ($C_2F_3^{35}Cl^+$), 97 ($C_2F_2^{35}Cl^+$), and 81 ($C_2F_3^+$) were observed at ~ 129 K (Figure 1). Possible parent molecules for these mass spectral fragments include C_2F_3Cl , $C_2F_3Cl_3$, and $C_2F_4Cl_2$. The absence of a peak at ~ 129 K for m/z 151 ($C_2F_3^{35}Cl_2^+$), a large fragment of both isomers of $C_2F_3Cl_3$,²² eliminates $C_2F_3Cl_3$ as a possibility. Similarly, the absence of a peak for m/z 135 ($C_2F_4^{35}Cl^+$) at ~ 129 K eliminates $C_2F_4Cl_2$ as a candidate. The observed mass spectral fragments for the desorption peak at ~ 129 K are consistent with the published mass spectrum of C_2F_3Cl .²² Moreover, the desorption temperature of the radiolytic product C_2F_3Cl is the same as that of CF_2Cl_2 (~ 129 K) and between that of C_2F_4 (~ 111 K) and $C_2F_4Cl_2$ (~ 136 K), consistent with the boiling point trend: C_2F_4 (198 K) < CF_2Cl_2 (243 K) \approx C_2F_3Cl (246 K) < $C_2F_4Cl_2$ (277 K).²² C_2F_3Cl has not been identified in γ -radiolysis studies.^{23,24}

C. Identification of 1,2-Dichloro-1,1,2,2-tetrafluoroethane (CF_2Cl-CF_2Cl). Postirradiation TPD data demonstrate the desorption of CF_2Cl-CF_2Cl at ~ 136 K, as described below (Figure 1). The desorption peak at ~ 136 K detected for m/z 135 corresponds to mass fragment $C_2^{37}Cl_3^+$ or $C_2F_4^{35}Cl^+$. The absence of a desorption feature for m/z 129 ($C_2^{35}Cl_3^+$) at ~ 136 K demonstrates that the peak for m/z 135 does not correspond to the mass spectral fragment $C_2^{37}Cl_3^+$, eliminating $C_2F_2Cl_4$ and $C_2F_3Cl_3$ as possible candidates. The absence of a peak for mass spectral fragment m/z 170 ($C_2F_4Cl_2^+$) at ~ 136 K does not rule out $C_2F_4Cl_2$ because $C_2F_4Cl_2$ does not have a parent peak.²² The presence of a small peak at ~ 136 K for m/z 151 ($C_2F_3^{35}Cl_2^+$) provides additional evidence for the identification of $C_2F_4Cl_2$, a species detected in γ -radiolysis studies of CF_2Cl_2 .^{23,24}

$C_2F_4Cl_2$ has two structural isomers, 1,2-dichloro-1,1,2,2-tetrafluoroethane (CF_2Cl-CF_2Cl) and 1,1-dichloro-1,2,2,2-tetrafluoroethane ($CFCl_2-CF_3$). Mass spectral data²² alone were not sufficient to distinguish between these two isomers. The radiolysis product identified as $C_2F_4Cl_2$ was attributed to the isomer CF_2Cl-CF_2Cl based on the fact that CF_2Cl-CF_2Cl would be more likely to form than CF_3-CFCl_2 because the formation of CF_3-CFCl_2 requires breaking two C-F bonds of CF_2Cl_2 compared to the formation of CF_2Cl-CF_2Cl , which requires breaking only one C-F bond. The absence of species containing five fluorine atoms provides additional evidence for the identification of the isomer CF_2Cl-CF_2Cl because if CF_3-CFCl_2 was produced, CF_3-CF_2Cl would also be produced.

The identification of $C_2F_4Cl_2$ as a radiolysis product is further corroborated by its desorption temperature (~ 136 K) being between that of C_2F_3Cl (~ 129 K) and $C_2F_2Cl_2$ (~ 147 K), consistent with the boiling point trends of the three species: C_2F_3Cl (246 K) < $C_2F_4Cl_2$ (277 K) < $C_2F_2Cl_2$ (295 K).²²

D. Identification of $C_2F_2Cl_2$. Desorption features for m/z 134 ($C_2F_2^{35}Cl^{37}Cl^+$), 132 ($C_2F_2^{35}Cl_2^+$), and 82 ($C^{35}Cl_2^+$) were detected at ~ 147 K in postirradiation temperature-programmed desorption experiments (Figure 1). The radiolysis products $C_2F_4Cl_2$, $C_2F_3Cl_3$, and $C_2F_2Cl_4$ were ruled out because desorption peaks for m/z 135 ($C_2F_4^{35}Cl^+$), 151 ($C_2F_3^{35}Cl_2^+$), and 167

($C_2F_2^{35}Cl_3^+$), large fragments of $C_2F_4Cl_2$, $C_2F_3Cl_3$, and $C_2F_2Cl_4$ respectively,²² were absent at ~ 147 K. The mass spectral fragments evincing desorption peaks at ~ 147 K are consistent with the published mass spectrum of $C_2F_2Cl_2$.²²

$C_2F_2Cl_2$ has three structural isomers: 1,1-dichloro-2,2-difluoroethene ($CF_2=CCl_2$), *trans*-1,2-dichloro-1,2-difluoroethene ($CFCl=CFCl$), and *cis*-1,2-dichloro-1,2-difluoroethene ($CFCl=CFCl$). $CF_2=CCl_2$ was rejected as a candidate because neither C_2FCl_3 ($CFCl=CCl_2$) nor C_2Cl_4 ($CCl_2=CCl_2$) was detected during postirradiation temperature-programmed desorption experiments. It was not possible to distinguish between the *cis* and *trans* isomers based on our experimental data.

Additional evidence to support the identification of $C_2F_2Cl_2$, not identified in γ -radiolysis studies,^{23,24} is provided by the desorption temperature (~ 147 K) of the radiolysis product $C_2F_2Cl_2$ being between the desorption temperatures of $C_2F_4Cl_2$ (~ 136 K) and $C_2F_3Cl_3$ (~ 152 K), consistent with the boiling point trend of the three species: $C_2F_4Cl_2$ (277 K) < $C_2F_2Cl_2$ (295 K) < $C_2F_3Cl_3$ (321 K).²²

E. Identification of 1,1,2-Trichloro-1,2,2-trifluoroethane ($CFCl_2-CF_2Cl$). The desorption peaks at ~ 152 K for m/z 151 ($C_2F_3^{35}Cl_2^+$) (Figure 1) and 153 ($C_2F_3^{35}Cl^{37}Cl^+$) correspond to mass spectral fragments of either $C_2F_3Cl_3$ or $C_2F_4Cl_2$. The absence of a peak for m/z 135 ($C_2F_4^{35}Cl^+$) at ~ 152 K demonstrates that the species desorbing at that temperature is $C_2F_3Cl_3$ and not $C_2F_4Cl_2$. Furthermore, desorption features for six additional mass spectral fragments of $C_2F_3Cl_3$ were detected at ~ 152 K: m/z 78 ($C_2F^{35}Cl_3^+$), 97 ($C_2F_2^{35}Cl_3^+$), 113 ($C_2F^{35}Cl_2^+$), 116 ($C_2F_3^{35}Cl^+$), and 167 ($C_2F_2^{35}Cl_3^+$).

We have assigned the $C_2F_3Cl_3$ mass spectral peaks to the 1,1,2-trichloro-1,2,2-trifluoroethane ($CFCl_2-CF_2Cl$) isomer and not the 1,1,1-trichloro-2,2,2-trifluoroethane (CF_3-CCl_3) isomer using arguments similar to those used in section C.

The identification of $C_2F_3Cl_3$ as a radiolysis product of CF_2Cl_2 is consistent with γ -radiolysis studies of CF_2Cl_2 .^{23,24} Moreover, the desorption temperature (~ 152 K) of $C_2F_3Cl_3$ is between that of $C_2F_2Cl_2$ (~ 147 K) and $C_2F_2Cl_4$ (~ 165 K), consistent with the boiling point trends: $C_2F_2Cl_2$ (295 K) < $C_2F_3Cl_3$ (321 K) < $C_2F_2Cl_4$ (366 K).²²

F. Identification of 1,1,2,2-Tetrachloro-1,2-difluoroethane ($CFCl_2-CFCl_2$). The postirradiation temperature-programmed desorption data evince peaks for fragments $C_2F_2^{35}Cl_3^+$ (m/z 167) (Figure 1), $C_2F_2^{35}Cl_2^{37}Cl^+$ (m/z 169), $C_2F^{35}Cl_3^+$ (m/z 148), $C_2F_2^{35}Cl^{37}Cl^+$ (m/z 134), $C_2F_2^{35}Cl_2^+$ (m/z 132), $C^{35}Cl_2^{37}Cl^+$ (m/z 119), $C^{35}Cl_3^+$ (m/z 117), $C_2F_2Cl^+$ (m/z 97), and $C^{35}Cl_2^+$ (m/z 82) at ~ 165 K. On the basis of comparison to published mass spectral data,²² we assign this desorption feature to $C_2F_2Cl_4$, a species not identified in γ -radiolysis studies of CF_2Cl_2 .^{23,24} The presence of a peak for m/z 148 ($C_2F^{35}Cl_3^+$) at ~ 165 K confirms the identification of $C_2F_2Cl_4$ because a peak for m/z 148 is absent in the published mass spectra of $C_2F_4Cl_2$ and $C_2F_3Cl_3$.²²

The $C_2F_2Cl_4$ mass spectral peaks were assigned to 1,1,2,2-tetrachloro-1,2-difluoroethane ($CFCl_2-CFCl_2$) and not 1,1,1,2-tetrachlorodifluoroethane (CCl_3-CF_2Cl) by using similar reasoning as that used in part C.

The identification of $C_2F_2Cl_4$ as a radiolysis product is further corroborated by its desorption temperature (~ 165 K) and boiling point (366 K)²² being the highest of all identified radiolysis products.

3.2. Dependence of Radiolysis Product Yield on Electron Fluence. To investigate the dependence of radiolysis product yield on electron fluence (the total number of electrons incident on the thin film), postirradiation temperature-programmed desorption experiments were conducted at constant electron

Dependence of Radiolysis Yield on Electron Fluence

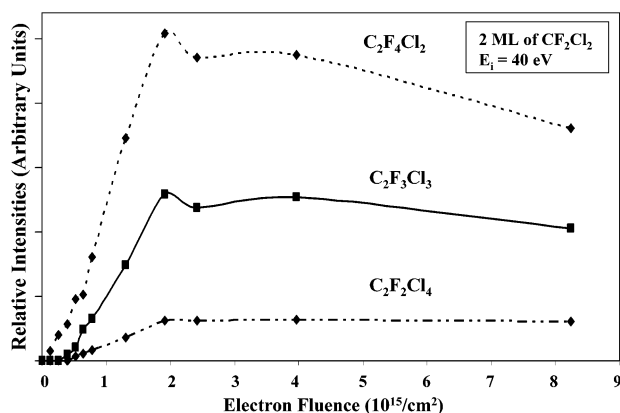
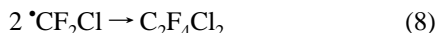
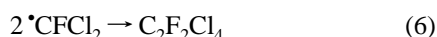
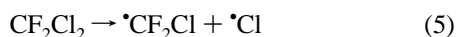
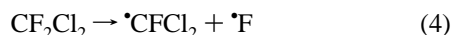


Figure 2. The radiolysis yield of C₂F₂Cl₄, C₂F₃Cl₃, and C₂F₄Cl₂ plotted as a function of incident electron exposure at a constant incident electron energy.

energy (40 eV) and film thickness (2 monolayers) while varying the electron fluence by changing the time of electron irradiation. The peaks for *m/z* 135 (C₂F₄Cl⁺), 151 (C₂F₃³⁵Cl₂⁺), and 167 (C₂F₂³⁵Cl₃⁺), major fragments of C₂F₄Cl₂, C₂F₃Cl₃, and C₂F₂Cl₄, respectively, at various electron fluences were integrated to quantify the product yield. As demonstrated in Figure 2, the radiolysis product yield increases with increasing electron fluence below a fluence of $1.3 \times 10^{15} \text{ cm}^{-2}$. The quadratic dependence on electron fluence (Figure 3) at low electron fluence is consistent with the radiolysis products being formed from products of two independent dissociation events. A mechanism involving radical formation (eqs 4 and 5) and radical–radical reactions (eqs 6–8) can be proposed based on this finding:



At fluences above $1.3 \times 10^{15} \text{ cm}^{-2}$, the radiolysis product yield remains approximately constant as the fluence is increased. On the basis of quantifying the amount of CF₂Cl₂ remaining in the thin film following electron irradiation, we attribute this finding to a significant fraction of CF₂Cl₂ being removed at an electron fluence of $\sim 1 \times 10^{15} \text{ cm}^{-2}$, and, hence, inhibiting the formation of radiolysis products.

3.3. Dependence of Radiolysis Product Yield on Electron Energy. The dependence of radiolysis product yield on electron energy was investigated by conducting postirradiation temperature-programmed desorption experiments at various electron energies (5–100 eV) at a constant electron fluence of $5 \times 10^{15} \text{ cm}^{-2}$ and a constant film thickness (2 monolayers). The electron fluence of the mass spectrometer was kept constant by adjusting the irradiation time to compensate for the change in incident electron flux with electron energy. The incident electron energy was varied by adjusting the voltage difference between the crystal and the mass spectrometer.

Radiolysis Yield at Low Electron Fluence

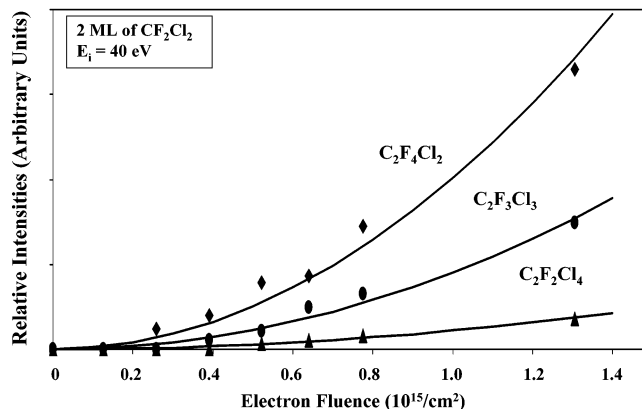


Figure 3. The radiolysis yield of C₂F₂Cl₄, C₂F₃Cl₃, and C₂F₄Cl₂ plotted as a function of incident electron exposure at low electron exposure.

Dependence of Radiolysis Yield on Electron Energy

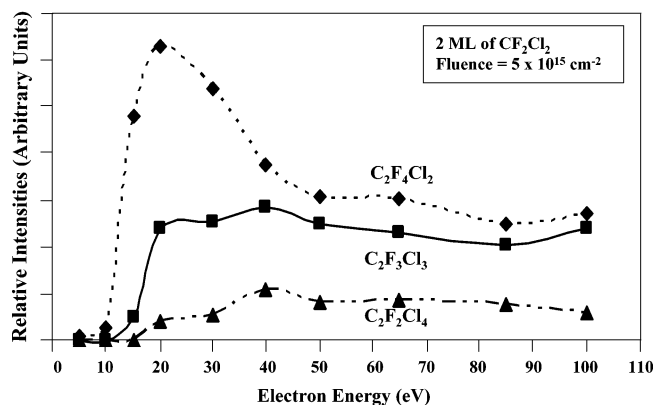


Figure 4. The radiolysis yield of C₂F₂Cl₄, C₂F₃Cl₃, and C₂F₄Cl₂ plotted as a function of incident electron energy at a constant electron exposure.

The plot of product yield as a function of electron energy (Figure 4) demonstrates that the radiolysis products C₂F₄Cl₂, C₂F₃Cl₃, and C₂F₂Cl₄ are only formed above an energy threshold of $\sim 10 \text{ eV}$. We attribute the miniscule amount of C₂F₄Cl₂ formed at an electron energy of $\sim 5 \text{ eV}$ to photochemically initiated reactions caused by photons emanating from the mass spectrometer filament during electron irradiation and during temperature-programmed desorption. The threshold behavior (Figure 4) suggests that electron impact excitation and/or ionization of CF₂Cl₂ is the first step in the reaction mechanism(s) producing $\cdot\text{CFCl}_2$ and $\cdot\text{CF}_2\text{Cl}$ radicals. However, our inability to extend our measurements to low electron energies precludes us from conclusively ruling out dissociative electron attachment, a process known to have a relatively large cross section below 5 eV for the production of Cl[−] (and $\cdot\text{CF}_2\text{Cl}$) and F[−] (and $\cdot\text{CFCl}_2$) from gas-phase CF₂Cl₂.² Because the ionization of CF₂Cl₂ at incident electron energies higher than $\sim 12 \text{ eV}$ can result in the production of very low energy electrons which may subsequently cause dissociative electron attachment of CF₂Cl₂, the radiolysis product yields as a function of electron energy may reflect the dependence of the ionization cross section on electron energy. A definitive conclusion regarding the role of very low energy electrons in the production of C₂F₄Cl₂, C₂F₃Cl₃, and C₂F₂Cl₄ via dissociative electron attachment of CF₂Cl₂ awaits additional experiments involving a monochromatic electron source with a significant electron flux at low electron energies.

Our experimental results of product yield versus electron energy (Figure 4) may demonstrate the role of electron attachment in the production of $\text{C}_2\text{F}_4\text{Cl}_2$ at higher electron energies. A recent study involving the electron-induced reactions of tetrahydrofuran, 3-hydroxytetrahydrofuran, and α -tetrahydrofurfuryl alcohol have identified resonance-like structures in the anion yield functions at electron energies as high as 23 eV.²⁵ This resonance-like behavior was attributed not to multiple electron scattering but to dipolar dissociation via capture into a transient anion state.²⁵ Such a mechanism may also explain our observation of a resonance-like structure in the postirradiation $\text{C}_2\text{F}_4\text{Cl}_2$ yield at ~ 20 eV (Figure 4).

3.4. Implications of Experimental Results. Our experimental findings suggest that the copious numbers of secondary low-energy electrons produced by cosmic rays could interact with stratospheric CF_2Cl_2 to produce $\text{C}_2\text{F}_3\text{Cl}_3$ (one of the seven most abundant chlorine-containing organic species found in the stratosphere)²⁶ and $\text{C}_2\text{F}_2\text{Cl}_4$ (not yet identified in the stratosphere). This reaction channel may play a role in the partitioning of Cl and F among source, sink, and reservoir gases in the stratosphere. Because the density of free electrons in the stratosphere is low, additional experiments involving the electron irradiation of CF_2Cl_2 adsorbed on ice are necessary to evaluate the importance of this new C–F bond cleavage channel.

We next discuss the implications of our findings for understanding the cosmic ray-induced production of Cl atoms that may subsequently destroy ozone in the stratosphere. This hypothesized reaction mechanism involves presolvated electrons whose energies are well below that of electrons used in our experiments for the production of CF_3Cl_3 and $\text{C}_2\text{F}_2\text{Cl}_4$. Hence the possible identification of new molecular species such as $\text{C}_2\text{F}_2\text{Cl}_4$ cannot “prove” the validity of the hypothesized cosmic ray-induced destruction of ozone in the stratosphere.

4. Conclusions

Electron-induced radiolysis reactions of condensed CF_2Cl_2 produce C_2F_4 , $\text{C}_2\text{F}_3\text{Cl}$, $\text{C}_2\text{F}_4\text{Cl}_2$, $\text{C}_2\text{F}_2\text{Cl}_2$, $\text{C}_2\text{F}_3\text{Cl}_3$, and $\text{C}_2\text{F}_2\text{Cl}_4$. In contrast to previous studies of *photon*-induced dissociation of CF_2Cl_2 , our studies of *electron*-induced dissociation demonstrate facile C–F bond cleavage in CF_2Cl_2 . This finding may have implications for understanding the partitioning of Cl and F among source, sink, and reservoir gases in the stratosphere.

Acknowledgment. C.R.A. gratefully acknowledges partial support from the donors of the Petroleum Research Fund, administered by the American Chemical Society, a Cottrell

College Science Award of the Research Corporation, a Henry-Dreyfus Teacher-Scholar award from the Camille and Henry Dreyfus Foundation, and a Brachman Hoffman fellowship from Wellesley College. Support for student researchers came from the Beckman Foundation, the National Science Foundation, and the Howard Hughes Medical Institute. The authors gratefully acknowledge several useful discussions with Professor David Haines (Wellesley College) and Dr. Andrew Bass (University of Sherbrooke).

References and Notes

- (1) Molina, M. J.; Rowland, R. D. *Nature* **1974**, *249*, 810.
- (2) Illenberger, E.; Scheunemann, H.-U.; Baumgartel, H. *Chem. Phys.* **1979**, *37*, 21–31.
- (3) Wayne, R. P. *Chemistry of Atmospheres*; Clarendon Press: Oxford, UK, 1985.
- (4) Lu, Q. B.; Madey, T. E. *J. Chem. Phys.* **1999**, *111*, 2861–2864.
- (5) Lu, Q. B.; Madey, T. E. *Phys. Rev. Lett.* **1999**, *82*, 4122–4125.
- (6) Lu, Q. B.; Madey, T. E. *Surf. Sci.* **2000**, *451*, 238–243.
- (7) Lu, Q.-B.; Madey, T. E. *J. Phys. Chem. B* **2001**, *105*, 2779–2784.
- (8) Lu, Q. B.; Sanche, L. *Phys. Rev. B: Condens. Matter Mater. Phys.* **2001**, *63*, 153403/1–153403/4.
- (9) Lu, Q. B.; Sanche, L. *Phys. Rev. Lett.* **2001**, *87*, 078501/1–078501/4.
- (10) Harris, N. R. P.; Farman, J. C.; Fahey, D. W. *Phys. Rev. Lett.* **2002**, *89*, 219801-1.
- (11) Sanche, L.; Lu, Q.-B. *Phys. Rev. Lett.* **2002**, *89*, 219802-1.
- (12) Muller, R. *Phys. Rev. Lett.* **2003**, *91*, 058502-1.
- (13) Christophorou, L. G.; Olthoff, J. K.; Wang, Y. *J. Phys. Chem. Ref. Data* **1997**, *26*, 1205–1237.
- (14) Denifl, G.; Muigg, D.; Walker, I.; Cicman, P.; Matejcik, S.; Skalny, J. D.; Stamatovic, A.; Mark, T. D. *Czech. J. Phys.* **1999**, *49*, 383–392.
- (15) Hedhili, M. N.; Lachgar, M.; Le Coat, Y.; Azria, R.; Tronc, M.; Lu, Q. B.; Madey, T. E. *J. Chem. Phys.* **2001**, *114*, 1844–1850.
- (16) Kiendler, A.; Matejcik, S.; Skalny, J. D.; Stamatovic, A.; Maerk, T. D. *J. Phys. B: At., Mol. Opt. Phys.* **1996**, *29*, 6217–6225.
- (17) Langer, J.; Matt, S.; Meinke, M.; Tegeder, P.; Stamatovic, A.; Illenberger, E. *J. Chem. Phys.* **2000**, *113*, 11063–11070.
- (18) Leiter, K.; Maerk, T. D. *Symp. Proc. Int. Symp. Plasma Chem., 7th* **1985**, *4*, 1325–1330.
- (19) Harris, T. D.; Lee, D. H.; Blumberg, M. Q.; Arumainayagam, C. R. *J. Phys. Chem.* **1995**, *99*, 9530–9435.
- (20) Fettweis, P.; Neve de Mevergnies, M. *J. Appl. Phys.* **1978**, *49*, 5699–5702.
- (21) Folcher, G.; Braun, W. *J. Photochem.* **1978**, *8*, 341–354.
- (22) NISTChemistry WebBook; NIST Standard Reference Database No. 69, March 2003 Release; National Institute of Standards and Technology: Gaithersburg, MD (<http://webbook.nist.gov>) (accessed March 2003).
- (23) Alfassi, Z. B.; Heusinger, H. *Radiat. Phys. Chem.* **1983**, *22*, 995–1000.
- (24) Alfassi, Z. B.; Mosseri, S.; Fuerst, W. *J. Radioanal. Nucl. Chem.* **1989**, *129*, 43–58.
- (25) Antic, D.; Parenteau, L.; Sanche, L. *J. Phys. Chem. B* **2000**, *104*, 4711–4716.
- (26) von Clarmann, T. L. A.; Oelhaf, H.; Fischer, H.; Friedl-Vallon, F.; Piesch, C.; Seefeldner, M.; Voelker, W.; Bauer, R.; et al. *J. Geophys. Res. [Atmospheres]* **1995**, *100*, 13, 979–997.